DISK SURFACE DENSITY TRANSITIONS AS PROTOPLANET TRAPS

F. S. MASSET[1,2]

Service d'Astrophysique, Orme des Merisiers, CE-Saclay, 91191 Gif-sur-Yvette Cedex, France; fmasset@cea.fr

A. MORBIDELLI AND A. CRIDA

Laboratoire Cassiopée, Centre National de la Recherche Scientifique, UMR 6202, Observatoire de la Côte d'Azur,
BP 4229, 06304 Nice Cedex 4, France; morby@obs-nice.fr, crida@obs-nice.fr

AND

J. FERREIRA

Laboratoire d'Astrophysique de Grenoble, 414 Rue de la piscine, BP 53, 38041 Grenoble Cedex 9, France;
jonathan.ferreira@obs.ujf-grenoble.fr

ABSTRACT

The tidal torque exerted by a protoplanetary disk with power-law surface density and temperature profiles onto an embedded protoplanetary embryo is generally a negative quantity that leads to the embryo inward migration. Here we investigate how the tidal torque balance is affected at a disk surface density radial jump. The jump has two consequences: (1) It affects the differential Lindblad torque. In particular, if the disk is merely empty on the inner side, the differential Lindblad torque almost amounts to the large negative outer Lindblad torque. (2) It affects the corotation torque, which is a quantity very sensitive to the local gradient of the disk surface density. In particular, if the disk is depleted on the inside and the jump occurs radially over a few pressure scale heights, the corotation torque is a positive quantity that is much larger than in a power-law disk. We show by means of customized numerical simulations of low-mass planets embedded in protoplanetary nebulae with a surface density jump that the second effect is dominant; that is, that the corotation torque largely dominates the differential Lindblad torque on the edge of a central depletion, even a shallow one. Namely, a disk surface density jump of about 50% over 3–5 disk thicknesses suffices to cancel out the total torque. As a consequence, the type I migration of low-mass objects reaching the jump should be halted, and all these objects should be trapped there provided some amount of dissipation is present in the disk to prevent the corotation torque saturation. As dissipation is provided by turbulence, which induces a jitter of the planet semimajor axis, we investigate under which conditions the trapping process overcomes the trend of turbulence to induce stochastic migration across the disk. We show that a cavity with a large outer to inner surface density ratio efficiently traps embryos from 1 to 15 $M_\oplus$, at any radius up to 5 AU from the central object, in a disk that has same surface density profile as the minimum mass solar nebula (MMSN). Shallow surface density transitions require light disks to efficiently trap embryos. In the case of the MMSN, this could happen in the very central parts ($r < 0.03$ AU). We discuss where in a protoplanetary disk one can expect a surface density jump. This effect could constitute a solution to the well-known problem that the buildup of the first protogiant solid core in a disk takes much longer than its type I migration toward the central object.

Subject headings: accretion, accretion disks — hydrodynamics — methods: numerical —
planetary systems: formation — planetary systems: protoplanetary disks

1. INTRODUCTION

The migration of low-mass protoplanets ($M_p < 15\ M_\oplus$) under the action of disk tides is long known to be a fast process in disks with power-law surface density profiles (Ward 1997; Tanaka et al. 2002). The fast migration timescale estimates of these objects even constitute a bottleneck for the core accretion scenario, which implies a slow buildup of a solid core until it reaches the mass threshold ($\sim 15\ M_\oplus$) above which rapid gas accretion begins. Indeed, the solid core buildup time is 10^6–10^7 yr (Pollack et al. 1996), while the migration timescale of a $M_p = 1\ M_\oplus$ planet is $O(10^5)$ yr (Ward 1997; Tanaka et al. 2002) and scales inversely proportionally to the planet mass. The existence of gaseous giant planets at large distances ($a \sim 0.1$–10 AU) from their central star therefore constitutes a puzzle. Recent work by Alibert

et al. (2005) has shown that the core buildup timescale can be lowered by taking migration into account, which prevents the depletion of the core feeding zone. However, these authors found that the most up-to-date type I migration timescale estimate, which includes three-dimensional effects and the corotation torque (Tanaka et al. 2002), still needs to be lowered by a factor of 10–100 in order to allow for the solid core survival. The total torque exerted by the disk onto the planet can be split into two parts: the differential Lindblad torque, which corresponds to the torque of the spiral wake that the planet excites in the disk, and the corotation torque, exerted by the material located in the planet co-orbital region. The role of the corotation torque has often been overlooked in migration rate estimates. The two main reasons for that are that it is harder to evaluate than the differential Lindblad torque and that it saturates (i.e., tends to zero) in the absence of dissipation. The corotation torque scales with the radial gradient of Σ/B, where Σ is the disk surface density and B is the second Oort's constant, or half the disk flow vorticity vertical component in a nonrotating frame. This scaling makes the corotation torque a

[1] Also at Instituto de Astronomia, Universidad Nacional Autónoma de México, Ciudad Universitaria, Apartado Postal 70-264, Mexico DF 04510, Mexico.

[2] Send offprint requests to: fmasset@cea.fr.

quantity very sensitive to local variations of the disk surface density or rotation profile. Here we investigate the behavior of the total (Lindblad + corotation) tidal torque exerted on a planet in the vicinity of a surface density radial jump in order to investigate a suggestion by Masset (2002) that localized, positive surface density jumps may be able to halt migration. We assume that the surface density transition occurs on a length scale λ of a few pressure scale heights H. We consider the case in which the surface density is larger on the outside of the transition, but we do not limit ourselves to the case in which the surface density on the inside is negligible compared to its value on the outer side. The case of a virtually empty central cavity has already been contemplated by Kuchner & Lecar (2002) in the context, different from ours, of giant planet migration. They concluded that giant planet migration is halted or considerably slowed down once the planet is inside the cavity and in 2:1 resonance with the cavity edge, as beyond this resonance the disk torque onto a planet on a circular orbit becomes negligible.

In § 2 we provide simple analytical estimates of the Lindblad and corotation torques at a surface density transition. We show that the corotation torque, which is a positive quantity there, is likely to overcome the Lindblad torque if the transition is localized enough, i.e., λ less than a few H. In § 3 we describe the numerical setup that we used to check this prediction with a numerical hydrocode. In § 4 we present the results of our numerical simulations, which indeed exhibit for a wide range of parameters a fixed point at the transition, i.e., a point where the corotation and Lindblad torques cancel each other and planetary migration stops. We also discuss in this section the issue of the saturation of the corotation torque and the need for turbulence to prevent it, and the conditions under which turbulence is able or unable to unlock a planet from the transition. We then discuss in § 5 where in protoplanetary disks such surface density transitions can be found and the consequences of these planet traps on giant planet formation.

2. A SIMPLE ANALYTIC ESTIMATE

A protoplanet embedded in a gaseous protoplanetary disk excites in the latter a one-armed spiral wake (Ogilvie & Lubow 2002) as a result of the constructive interference of propagative density waves excited at Lindblad resonances with the planet. This wake exerts a torque on the planet, which can be decomposed into the outer Lindblad torque (Γ_o), which is negative, and is exerted by the outer arm, and the inner Lindblad torque (Γ_i), which is positive and is exerted by the inner arm. These two torques do not cancel out. The residue $\Delta\Gamma = \Gamma_o + \Gamma_i$, called the differential Lindblad torque, is negative (Ward 1986), thereby leading to inward migration. If one calls one-sided Lindblad torque the arithmetic mean of the absolute values of the outer and inner Lindblad torques,

$$\Gamma_{\mathrm{LR}} = \frac{\Gamma_i - \Gamma_o}{2}, \tag{1}$$

then the differential Lindblad torque is a fraction of this torque that scales with the disk aspect ratio $h = H/r$, where H is the pressure scale height or disk thickness and r is the radius. In particular, for a disk with uniform surface density and aspect ratio (Ward 1997),

$$\Delta\Gamma \approx -8h\Gamma_{\mathrm{LR}}. \tag{2}$$

As noted by Ward (1997), in a nebula with $h = O(10^{-1})$, the differential Lindblad torque is a sizable fraction of the one-sided

Lindblad torque. This is of some importance for our concern: denoting $\Delta\Gamma'$ the Lindblad torque on an empty cavity edge (it then amounts to the outer Lindblad torque, i.e., $\Delta\Gamma' = \Gamma_o$) and $\Delta\Gamma$ the Lindblad torque farther out in the disk where we assume the surface density and aspect ratio profiles to be flat, we have

$$\Delta\Gamma' \approx \Delta\Gamma/(8h), \tag{3}$$

which means that the Lindblad torque on a cavity edge is at most 2–3 times larger than farther out in the disk, for $0.04 < h < 0.06$.

In addition to the wake torque, the material in the orbit vicinity exerts on the planet the so-called corotation torque. This torque scales with the gradient of the specific vorticity (or vortensity) (Goldreich & Tremaine 1979; Ward 1991, 1992):

$$\Gamma_C \propto \Sigma \, \frac{d \log (\Sigma/B)}{d \log r}. \tag{4}$$

This torque comes from the exchange of angular momentum between the planet and fluid elements that perform U-turns at the end of their horseshoe streamlines (Ward 1991; Masset 2001, 2002). It has been estimated that the corotation torque amounts to a few tens of percent (Korycansky & Pollack 1993) of the differential Lindblad torque for a disk with a power-law surface density profile. Tanaka et al. (2002) give the following estimate for a three-dimensional disk with flat surface density and temperature profiles:

$$\Gamma_C \approx -(1/2)\Delta\Gamma. \tag{5}$$

Note that the corotation torque cancels out for a surface density profile $\Sigma \propto r^{-3/2}$, while it is a positive quantity for a shallower surface density profile.

We now estimate the ratio of the corotation torque at a cavity edge and farther out in the disk (assuming a flat surface density profile). We assume that the surface density inside of the transition is Σ_i, while it is $\Sigma_o > \Sigma_i$ on the outside. The transition from Σ_i to Σ_o occurs on a length scale $\lambda \ll r$. In the outer disk where $\Sigma \equiv \Sigma_o$, we have

$$\frac{d \log (\Sigma/B)}{d \log r} = 3/2, \tag{6}$$

while at the transition, $d \log \Sigma / d \log r$ is a sharply peaked function with a maximum that scales as

$$\left| \frac{d \log \Sigma}{d \log r} \right|_{\max} \sim \frac{r}{\lambda} \, \log\!\left(\frac{\Sigma_o}{\Sigma_i} \right). \tag{7}$$

Similarly, retaining only the terms that vary most rapidly with r at the transition:

$$\frac{d \log B}{d \log r} \simeq \frac{2r^2}{\Omega} \frac{d^2\Omega}{dr^2}, \tag{8}$$

where Ω is the angular velocity. The last factor of the above equation can also be expressed, using the disk rotational equilibrium and again keeping only the terms that vary most rapidly with r, as

$$\frac{d^2\Omega}{dr^2} \simeq -\frac{\Omega h^2 r}{2} \frac{d^3 \log \Sigma}{dr^3}. \tag{9}$$

The last factor of the right-hand side is a function of r that scales as $(H^2 r/\lambda^3) \log (\Sigma_o/\Sigma_i)$, and that has, for a sufficiently smooth,

monotonic transition from Σ_i to Σ_o, two minima and one maximum, the exact locations and amplitudes of which depend on the surface density profile. The (inverse of) the specific vorticity logarithmic gradient is therefore

$$\frac{d \log(\Sigma/B)}{d \log r} = \frac{r}{\lambda} \log\left(\frac{\Sigma_o}{\Sigma_i}\right)\left(a + b \frac{H^2}{\lambda^2}\right), \qquad (10)$$

where a and b are numerical functions of r of order unity that depend on the exact shape of the surface density profile. In particular, one sees immediately that if $\lambda \sim H$, then the contributions of both terms (the surface density gradient and the vorticity gradient) to the corotation torque are of similar magnitude.

The corotation torque at the transition Γ'_C can therefore be larger than the corotation torque Γ_C farther out in the disk by a factor

$$\frac{\Gamma'_C}{\Gamma_C} \approx \frac{2r}{3\lambda} C, \qquad (11)$$

where C is a numerical factor of order unity that depends on the surface density profile.

Using equations (3), (5), and (11), we find that

$$\frac{\Gamma'_C}{\Delta\Gamma'} \approx -\frac{8H}{3\lambda} C, \qquad (12)$$

which means that the (positive) corotation torque can counteract the (negative) Lindblad torque at a cavity, provided that the edge of the latter be narrow enough ($\lambda < 8HC/3$). We check by means of numerical simulations that it is indeed possible to halt type I migration on the edge of a surface density transition.

3. NUMERICAL SETUP

We performed a large number of two-dimensional hydrodynamic simulations that we detail below. The code used was FARGO.[3] It is a staggered mesh code on a polar grid, with upwind transport and a harmonic, second-order slope limiter (van Leer 1977). It also uses a change of rotating frame on each ring that enables one to increase the time step significantly (Masset 2000a, 2000b).

The surface density transition was set in the following manner. We call F the target surface density ratio between the inside and the outside of the cavity: $F = \Sigma_o/\Sigma_i$. In order to realize this ratio, we adopt a fixed profile of kinematic viscosity with an inverse ratio: $\nu_o/\nu_i = F^{-1}$. If we call r_t the mean radius of the transition, then for $r > r_t + \lambda/2$, $\nu \equiv \nu_o$; for $r < r_t - \lambda/2$, $\nu \equiv \nu_i$; and for $r_t - \lambda/2 < r < r_t + \lambda/2$, ν is an affine function of r. We then relax the surface density profile during a preliminary one-dimensional calculation over $\sim 10^5$ orbits, so that the profile can safely be considered as steady state in the two-dimensional calculations. In our calculations we use nonreflecting inner and outer boundary conditions, while we impose the disk surface density at the inner and outer boundary.

In all our calculations the disk aspect ratio is $h = 0.05$, the disk is not self-gravitating, and it has a locally isothermal equation of state. The length unit is r_t. The mesh inner and outer boundaries are at $r = 0.42$ and 2.1, respectively. The mass unit is the mass M_* of the central object, and the gravitational constant is $G = 1$. The time unit is $(GM_*/r_t^3)^{-1/2}$. Whenever we quote a planet mass in Earth masses, we assume the central object to have a solar mass.

[3] See http://www.maths.qmul.ac.uk/~masset/fargo.

The mesh size in all our runs is $N_r = 168$ and $N_\phi = 450$; hence, the radial resolution is 10^{-2}. The horseshoe zone width for a 15 $M_\oplus$ planet is $\sim 7.8 \times 10^{-2}$, so it is approximately eight zones wide. The error on the corotation torque due to this finite width therefore amounts to at most $\sim 10\%$ (see Masset 2002; their Fig. A.3). We also made calculations with a 4 $M_\oplus$ mass planet for which the horseshoe zone is only four zones wide. This resolution may seem low, but the corotation torque is very well captured at low resolution for small-mass planets that hardly perturb the surface density profile (see discussion in Masset 2002; their Appendix A).

We contemplated the fashionable issue of whether the Roche lobe content must be included or not when integrating the torque over the disk material (D'Angelo et al. 2005; Masset & Papaloizou 2003). We found that taking that material into account or not makes essentially no difference in our case. We make the following technical comments related to this issue:

1. D'Angelo et al. (2005) have envisaged the case of Jupiter- or Saturn-mass planets, for which there is a significant Roche lobe with radius $\sim a(M_p/3M_*)^{1/3}$ (a being the planet semimajor axis). For the mass range studied here ($M_p < 15\,M_\oplus$), the Roche lobe size is much smaller than this simple estimate. In particular, in the linear limit, the flow does not exhibit any circumplanetary libration, while the two ends of the horseshoe region reconnect through a single stagnation point located on the orbit (F. S. Masset et al. 2006, in preparation; H. Tanaka 2005, private communication), which is offset from the planet as a result of the gaseous disk slight sub-Keplerianity. The issue of Roche lobe sampling in that case is therefore irrelevant.

2. D'Angelo et al. (2005) have found that resolution may alter the torque exerted on the planet when the Roche lobe material is taken into account. This behavior, which appears at very high resolution, is related to the buildup of a gaseous envelope around the pointlike planet, while the mass of this envelope depends heavily on the equation of state, which is poorly known. The envelope mass may be considerable for the giant protoplanets considered by D'Angelo et al. (2005), as it may be several times the planet mass, but it is presumably a much smaller fraction of the planet mass for the planet masses that we consider ($M_p < 15\,M_\oplus$; see also Alibert et al. 2005).

In two-dimensional simulations one has to introduce a potential smoothing length ϵ meant to mimic the disk vertical extent. The planet potential expression is then $-GM_p/(r^2 + \epsilon^2)^{1/2}$, where G is the gravitational constant and r is the distance to the planet. In our calculations we use a potential smoothing length $\epsilon = 0.7H$. This is quite a large value, which leads to underestimate the corotation torque (Masset 2002), as it lowers the horseshoe zone width, while the corotation torque is proportional to the fourth power of this width. Our calculations are therefore conservative, and it is likely that three-dimensional calculations would yield a torque cancellation for an even wider set of disk parameters than we found.

4. RESULTS OF NUMERICAL SIMULATIONS

4.1. *Torque Sampling on a Cavity Edge*

We consider in this section a disk with a target surface density ratio between the inside and the outside of the transition set to $F = 7$. As this value is large compared to 1, we call the inside part of the transition a cavity. We performed two sequences of 75 calculations in which a planet was set on a fixed circular orbit with radius $a_i = 0.65 + 10^{-2}i$ ($i = 0 \ldots 74$). For these calculations we report as a function of a_i the total torque exerted on the
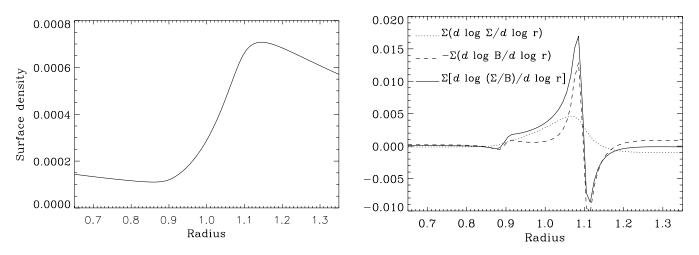
Fig. 1.—*Left*: Surface density profile for the runs of § 4.1. The surface density transition occurs over ∼4H, between $r \approx 0.9$ and 1.1. *Right*: Corresponding profiles of the different logarithmic derivatives involved in the expression of the corotation torque, weighted by the surface density. The dotted line shows the logarithmic derivative of the surface density, the dashed line shows the opposite of the logarithmic derivative of the flow vorticity, and the solid line shows the sum of these two quantities. It corresponds to the right-hand side of eq. (4).

planet (averaged over 100 orbits, in order for the libration flow inside the co-orbital region to reach a steady state; Masset 2002).

The left plot of Figure 1 shows the relaxed surface density profile after 10^5 orbits of the preliminary one-dimensional calculation, and the right plot shows the quantities involved in the corotation torque scaling. The right panel of Figure 1 shows that the vortensity gradient peak is only partially due to the surface density gradient, since the gradient of the flow vorticity plays a role of comparable importance, as suggested in § 2.

The total torque measured from numerical simulations is presented in Figure 2. Both plots, which correspond to two different planet masses, exhibit similar features:

1. On the left side (for $r < 0.8$) and on the right side (for $r > 1.2$), the torque profile is flat and negative. This corresponds to the total negative torque acting on a planet embedded in a flat surface density disk. Since the surface density is $F = 7$ times lower on the inside, the torque value is much smaller on that side.

2. In the range $0.8 < r < 1.2$, the torque as a function of radius exhibits a shape very similar to the vortensity gradient shown in Figure 1. In particular, the torque has a maximum value near $r = 1.08 - 1.10$ and a minimum value near $r = 1.12 - 1.13$.

This last observation unambiguously indicates that the corotation torque largely dominates the total torque at the surface density transition, as expected from the analytic estimate. In

particular, there are two positions in the disk where the total torque cancels out (and therefore where the migration is halted): one at $r \approx 0.92$ and the other at $r \approx 1.11 - 1.12$. The first of these fixed points is unstable: moving the planet away from it yields a torque that moves it farther away, while the second one (i.e., the outermost one) is stable: moving the planet to a higher radius yields a negative torque that tends to bring the planet back to its former position, and vice versa for a motion toward smaller radii. The fixed point at $r = 1.12$ should therefore trap all type I migrating embryos. We note in passing that the torque as a function of radius does not have exactly the same shape between a 15 and a 4 $M_\oplus$ planet. There are two reasons for this: the onset of nonlinear effects between 4 and 15 $M_\oplus$, and the inaccuracy of the corotation torque estimate for the 4 $M_\oplus$ case, for the resolution that we have adopted. However, we see that even in the 4 $M_\oplus$ case, the value of the torque maximum ($\sim 6 \times 10^{-5}$) is much larger than the torque absolute value away from the cavity (for $r > 1.2$, this value is $\sim 10^{-5}$). Therefore, even if the error on the corotation torque amounts to 50% (see Masset 2002), one still gets a torque cancellation and a stable fixed point.

4.2. *Halting Migration at a Cavity Edge*

We have performed a series of 10 calculations with planets of masses 1.3–15 $M_\oplus$ in geometric sequence, with the same disk
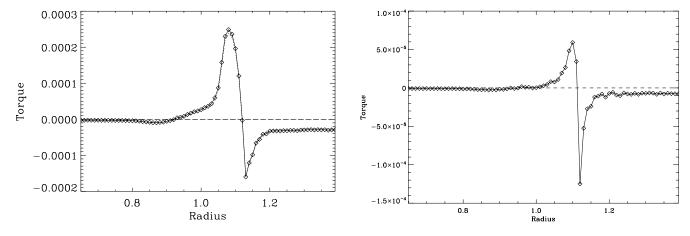

Fig. 2.—*Left*: Specific torque acting on a 15 $M_\oplus$ planet on a fixed circular orbit, as a function of its orbital radius. *Right*: Same, but for a 4 $M_\oplus$ planet.
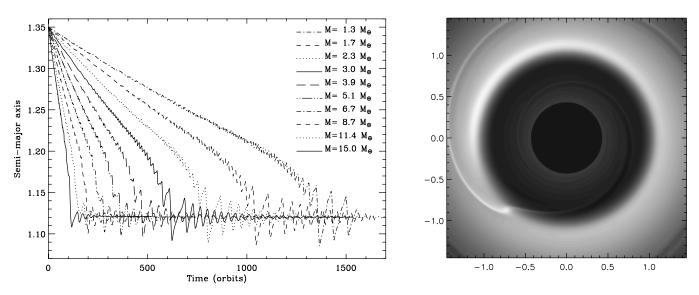
Fig. 3.—*Left*: Primary to planet separation curve as a function of time, for the 10 different planet masses. *Right*: Snapshot of the surface density map with a 15 $M_\oplus$ planet embedded at $t = 480$ orbits.

cavity as in the previous section ($F = 7$). In these calculations the planets were released at $r = 1.35$, i.e., beyond the cavity edge, and then allowed to freely migrate under the action of the disk torque. The results are presented in Figure 3. We see how the transition efficiently traps all these objects at the fixed point at $r = 1.12$ identified in the previous section. We note in passing that on the lower side of the mass range considered, the small width of the horseshoe region may lead to large uncertainties on the corotation torque. Nevertheless, the migration of all objects stops at locations that are all very close to 1.12. This indicates that the corotation torque at the edge, even misrepresented by a too low resolution, still strongly dominates the differential Lindblad torque. For masses lower than a few Earth masses, the Hill radius is much smaller than the disk thickness, and the disk response is linear. In the linear regime, the corotation to Lindblad torque ratio is independent of the planet mass. As we have stressed already, our potential smoothing length is large, and our corotation torque estimate is conservative. This indicates that any small-mass infalling embryo will be trapped at the cavity edge that we modeled.

Disk profiles with an extremum of the specific vorticity are prone to a linear Rossby wave instability that eventually leads to

the formation of vortices (Li et al. 2000, 2001). This is the case of the transitions that we have simulated. The arc-shaped overdense region located near $x = -0.5$, $y = +0.5$ in the right plot of Figure 3 corresponds to such a vortex. It leads to a torque modulation over the synodic period between the planet and the vortex, which is seen on the migration curves of the left plot of Figure 3. As a planet approaches the transition, the synodic period increases, and so does the period of the semimajor axis modulations.

4.3. *Torque Sampling at a Shallow Surface Density Jump*

We have performed a series of calculations similar to those of § 4.1, except that we adopted a much smaller target outer to inner surface density ratio: $F = 1.4$ instead of 7. The surface density jump is therefore a very shallow one. The results are presented in Figure 4. They show that again there is a fixed point at which migration is halted, at $r \approx 1.09$. We have not searched further the limit inner to outer surface density ratio that leads to migration reversal, as this quantity depends on the jump radial size, on the profile adopted for the kinematic viscosity, and on the potential smoothing length. We just stress that a factor $F = 1 + O(1)$ and a jump size of $\sim 4H$ suffice to halt migrating bodies.
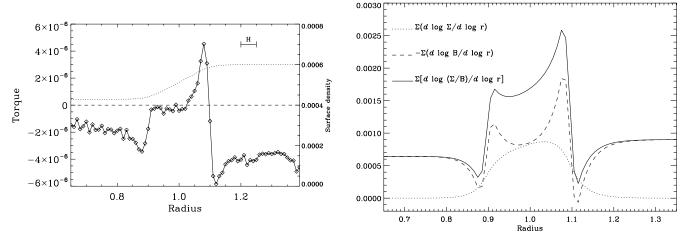

Fig. 4.—*Left*: Surface density profile for the runs of § 4.3 (*dotted line and right axis*) and total torque exerted by the disk on the planet as a function of its semimajor axis (*diamonds and left axis*), for a 4 $M_\oplus$ planet. *Right*: Corresponding profiles of the different logarithmic derivatives involved in the expression of the corotation torque, weighted by the surface density, as in Fig. 1.

4.4. Driving of Trapped Planets

As can be seen in Figure 2 or 4, the torque maximum value is positive and large. This implies that, if the cavity radius evolves with time, either inward or outward, it drives any planet trapped on its edge so that its migration follows the edge evolution. More precisely, a planet will be held at a location where the specific torque acting on it endows it with a drift rate equal to that of the cavity radius. As the torque maximum in absolute value is at least of the order of the total torque in the outer disk, this means that the edge expansion or contraction can be as fast as the type I drift rate of its trapped objects and still keep these objects trapped. We illustrate this shepherding in Figure 5. We performed a calculation in which an initially fixed cavity, such as the one considered at the previous sections (here with $F = 10$ and a transition over $4H$–$5H$), traps a $15\ M_\oplus$ infalling planet and then is endowed with an expansion rate $\dot{r}_t = 8 \times 10^{-5}$. This is achieved by imposing a kinematic viscosity profile as described in § 3 with a radius r_t that varies linearly with time. One can see that the planet semimajor axis follows the cavity radius evolution, so that the planet remains trapped on the cavity edge.

4.5. Dissipation and Corotation Torque Saturation

4.5.1. Corotation Torque Saturation

The corotation torque, in the absence of any angular momentum exchange between the horseshoe region and the rest of the disk, is prone to saturation: its value tends to zero after a few libration periods (Ward 1991, 1992; Masset 2001, 2002; Balmforth & Korycansky 2001). The disk turbulence, which endows the disk with an effective viscosity, can help to prevent the corotation torque saturation. Here we estimate the amount of viscosity required to prevent saturation, as a function of the planet mass. The maximal amount of saturation for which one still has a torque cancellation depends on the planet mass and on the detailed disk profiles. Here we just give an order of magnitude of the viscosity needed to prevent saturation by assuming a 50% saturation. This amount of saturation is reached when the viscous timescale across the horseshoe region is equal to the horseshoe libration timescale (Masset 2001):

$$\frac{x_s^2}{3\nu} = \frac{4\pi a}{(3/2)\Omega_p x_s}, \qquad (13)$$

where x_s is the horseshoe zone half-width, ν is the disk effective kinematic viscosity, Ω_p is the planet orbital frequency, and a its semimajor axis. In order to express x_s as a function of the planet mass,[4] we note that in the linear (hence fully unsaturated) limit the corotation torque can be expressed as (Ward 1991; Masset 2001)

$$\Gamma_C = \frac{9}{8} x_s^4 \Omega_p^2 \Sigma, \qquad (14)$$

while from Tanaka et al. (2002) we have

$$\Gamma_C = 0.939 h^{-2} q^2 a^4 \Omega_p^2 \Sigma, \qquad (15)$$

where $q = M_p/M_*$. Equations (14) and (15) yield

$$x_s = 0.96 a \sqrt{\frac{q}{h}}. \qquad (16)$$

[4] The estimate provided here is given for a flat surface density profile, but the horseshoe region width should not, or very weakly, depend on this assumption.
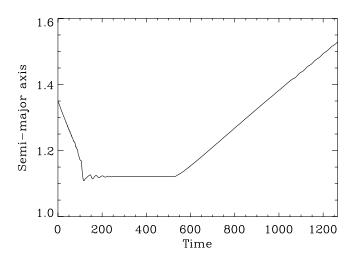

Fig. 5.—Semimajor axis as a function of time for a planet trapped in an expanding cavity. The cavity is fixed for the first 520 orbits, then is linearly expanding with time. The planet semimajor axis follows the cavity evolution so that the planet remains trapped at the cavity edge. At $t = 0$ the planet is released beyond the cavity, at $r = 1.35$. During the first 100 orbits it migrates toward the cavity, where it gets trapped.

Equations (13) and (16) give the minimum effective viscosity to prevent the corotation torque saturation:

$$\nu = 0.035 \left(\frac{q}{h}\right)^{3/2} a^2 \Omega_p, \qquad (17)$$

or, in terms of the α-coefficient ($\nu = \alpha H^2 \Omega_p$):

$$\alpha = 0.035 q^{3/2} h^{-7/2} = 6.5 \times 10^{-6} \left(\frac{M_p}{1\ M_\oplus}\right)^{3/2} \left(\frac{h}{0.05}\right)^{-7/2}. \qquad (18)$$

The value of α required to prevent the corotation torque saturation of an Earth-mass planet is therefore much smaller than the one inferred from disk lifetimes of T Tauri stars, namely, $\alpha = 10^{-3}$ to 10^{-2} (Hartmann 2001). Note that this also holds for large-mass solid cores ($M_p = 10$–$15\ M_\oplus$). The corotation torque acting on these objects should therefore be a large fraction of the unsaturated estimate, so the analysis presented above for the torque cancellation is essentially valid. We also note that the planets of Figures 3 and 5 remain trapped over a timescale much longer than the horseshoe libration timescale, so that their corotation torque partial saturation is weak enough. The disk effective viscosity at the trap location is in these calculations 5×10^{-6} (i.e., $\alpha = 2 \times 10^{-3}$).

We remark that the corotation torque saturation could be different in a laminar disk with kinematic viscosity ν and in a turbulent disk (we discuss this topic in more detail in the next section) with the same effective viscosity, when the horseshoe region width is smaller than the turbulence length scale. The saturation should be easier to remove in this last case, which suggests that our saturation estimate is a conservative one.

4.5.2. Dissipation and Turbulence

Since the likely physical origin of the disk effective viscosity is turbulence, in particular, the turbulence generated by the magnetorotational instability (MRI; Balbus & Hawley 1991), the torque acting on the planet does not have a value constant in time as in a laminar disk, but rather displays large temporal fluctuations arising from the density perturbations in the planet vicinity.

It is important to assess the impact of these fluctuations on the mechanism outlined here. In the bulk of a disk with a smooth surface density profile, these torque fluctuations can yield an erratic behavior of the planet semimajor axis referred to as "stochastic migration" (Nelson & Papaloizou 2004; Nelson 2005). In what follows we use the torque fluctuation estimates of Nelson & Papaloizou (2004) and Nelson (2005) in order to determine whether despite its semimajor axis jitter the planet is confined to the trap vicinity, or whether it is unlocked from the trap position. We use a very simple prescription, which we detail in the Appendix, to perform Monte Carlo calculations of the planet semimajor axis over a period of time $t = 10^7 \, \Omega^{-1}$. We place initially the planet at the outer stable fixed point, and we declare it trapped if, over that amount of time, it never goes through the inner, unstable fixed point, while we declare it not trapped if it happens to go through the inner fixed point. While the Appendix presents the technical details of our calculations, we discuss below a number of issues relevant to these calculations.

1. Can the torque acting on the planet be considered as the sum of the torque in a laminar disk and the fluctuations arising from turbulence? Nelson (2005) found that this might not be the case, at least as long as the differential Lindblad torque is concerned, since the corotation region is not sufficiently resolved in his calculations; as an alternative explanation to the lack of the torque convergence to the laminar value, Nelson (2005) suggested the existence of very low frequency components of the torque fluctuations. As this problem is essentially open (and totally unaddressed as far as the corotation torque is concerned), we chose to describe the torque acting on the planet by the sum of the torque in the laminar case and of the torque fluctuations due to the turbulence.

2. The amplitude A of the torque fluctuations can be estimated by considering a density fluctuation of order unity with a length scale of order H, at a distance H from the planet (Nelson & Papaloizou 2004; Nelson 2005) and found to amount to $A = G\Sigma r$, where G is the gravity constant and r is the distance to the central object. This is the value that we adopt for our calculations.

3. The timescale of the fluctuations is of particular importance to assess the torque convergence toward its laminar value. Nelson (2005) found in his calculations that the torque fluctuations due to turbulence contain significant power at very low frequency and suggested that this could be linked to global communication across the disk on the viscous timescale. Here our situation is rather different, as the planet lies on a radially localized structure, with a radial extent λ. Fluctuations with frequency lower than $\sim \lambda/c_s$ would imply turbulent structures larger than the trap width and therefore would imply a radial displacement of the trap itself along the lines of § 4.4. Here we choose a correlation timescale for the turbulence of $t_c = 8\Omega^{-1} \sim 2\lambda/c_s$ for $\lambda \sim 4H$.

4. Both the tidal torque and the torque fluctuations scale with the disk surface density, so that the time needed for the time-averaged torque to reach convergence does not depend on the latter. However, the spread of the probability density of the planet semimajor axis after that timescale does depend on the disk surface density. If the expectancy of the distance of the planet to its initial location is larger than the trap width, then the planet can certainly be lost, while if it is much smaller than the trap width, the planet is certainly trapped. Our study therefore amounts to a disk critical mass search. For a given trap profile, a given planet mass and given fluctuation characteristics $A \propto \Sigma$ and t_c, there exists a critical disk mass so that a lighter disk keeps the planet trapped,
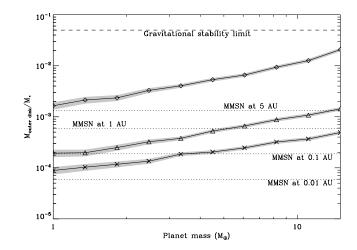

FIG. 6.—Critical disk mass as a function of the planet mass (from 1 to 15 $M_\oplus$), for different transition profiles: the $F = 7$ cavity of § 4.1 (*diamonds*) and the $F = 1.4$ shallow jump of § 4.3 (*crosses*). The triangles represent the trapping limit for a torque curve with a peak maximum, which is the geometric mean of the peak values of the $F = 7$ and $F = 1.4$ transitions, which we assume to be representative of a transition with $F \simeq 1 + (0.4 \times 6)^{1/2} = 2.5$. The dotted lines show the MMSN relative mass (as defined by its local surface density) at different radii. The thickness of the gray line indicates the results standard deviation found with different random seeds.

while a heavier disk is unable to lock it, and the planet is likely to go through the inner unstable fixed point. We perform this search in a dichotomic manner until we reach a precision of 5% on the disk mass, and we repeat the calculation with different random seeds, so as to get an idea of the precision on the disk critical mass estimate. Our results are displayed in Figure 6. The "disk outer mass" is defined as $M_{\text{outer disk}} = \pi r_t^2 \Sigma_{\text{out}}$, where Σ_{out} is the disk surface density on the outside of the surface density transition. We see in this figure that the deep cavity with $F = 7$ unconditionally traps $M = 1$–15 $M_\oplus$ protoplanets in a disk with a density profile of the MMSN, at any distance up to $\sim$5 AU, while the shallow surface density transition would be able to retain in falling bodies only in the very central regions ($r_t \simeq 0.01$ AU, if the nebula extends that far in) of such a nebula. Farther out in the disk, at $r = 0.1$ AU, a shallow transition in the MMSN would only capture embryos with $M > 4 \, M_\oplus$, etc.

It is not unreasonable to assume that these simple calculations are conservative, for the following reasons:

1. We have assumed the torque fluctuations to scale only with the disk surface density, which implies that all the disk material in the trap vicinity is turbulent. There is at least one realization of the trap, which is the inner edge of a dead zone (detailed in the next section), for which this statement is wrong. In our example, the trap stable fixed point corresponds to a location with a large surface density, therefore located rather on the "dead" side of the transition, i.e., where turbulent transport of angular momentum is inefficient and hence where the turbulence should be much weaker than contemplated in our simple Monte Carlo calculations.

2. We recall that our large potential smoothing length tends to significantly underestimate the corotation torque, while the trap ability to lock infilling bodies, for a given turbulence characteristics, strongly depends on the corotation torque peak value at the surface density transition.

We conclude this section with two remarks. First, the numerical simulations undertaken by Nelson & Papaloizou (2004) and Nelson (2005) neglect, for reasons of computational speed, the

gravitational potential z-dependency, which means that their disks have no vertical stratification. Future numerical experiments with vertical stratification may lead to different characteristics of the torque fluctuations. Second, other sources of turbulence have been suggested in protoplanetary disks, such as the global baroclinic instability (Klahr 2004), which may have different torque fluctuations statistics, and for which the trap efficiency may therefore be different. To date this is essentially an unaddressed issue.

5. DISCUSSION

The mechanism exhibited here is generic, since it plays a role at any positive disk surface density transition, even shallow ones, with the cautionary remark that some turbulence is required to prevent the corotation torque saturation, and that a condition is required on the disk mass to prevent the stochastic migration induced by the turbulence to overcome the trap effect. Although our knowledge of the detailed properties of protoplanetary disks is still incipient, we already know a number of locations for transitions exhibiting the above properties, which constitute potential traps for infalling embryos:

1. At the inner edge of a dead zone (Gammie 1996; Fromang et al. 2002), the surface density is expected to be significantly larger in the dead zone than in the ionized inner disk, while the inner disk turbulence provides the dissipation required to maintain the corotation torque. If the dead zone inner radius changes with time (since layered accretion involving a dead zone is thought not to be a steady process), then the objects trapped at the fixed point follow the transition radius, as shown in § 4.4. The edges of dead zones are thought, in the totally different context of runaway or type III migration (Masset & Papaloizou 2003), to be able to halt or reverse a runaway episode (Artymowicz 2004). Here, in our context of small-mass, type I migrating objects, we argue that the inner edge of a dead zone halts type I migrating bodies and efficiently traps them.

2. Sizable surface density transitions can also be found at the transition between an inner disk region where jets are launched and the outer viscous disk (Ferreira & Pelletier 1995). Indeed, the accretion velocity in the jet-emitting disk (JED) region is entirely due to the jet torque and becomes much larger than in a standard accretion disk (SAD). Mass flux conservation then leads to a surface density jump at the transition radius between the SAD and the JED. This radius has been inferred to vary from 0.3 to a few AU in some T Tauri stars[5] (Coffey et al. 2004; Pesenti et al. 2004). As all known embedded objects have jets, the existence of such a transition radius provides a natural trap for infalling embryos over the jet lifetime.

3. We finally mention the outer edge of a gap opened by a preexisting giant protoplanet. The latter can trap planetesimals at mean motion resonances (Hahn & Ward 1996) and also at the large positive surface density gradient found on its gap outer edge.

We note that the first two possibilities might not coexist in an accretion disk. Not all T Tauri stars show indeed evidence of high-velocity jets (Hartigan et al. 1995). For these jetless stars, the whole disk is likely to resemble a SAD with a dead zone in its innermost region. The protoplanet trap would then be realized at the inner radius of the dead zone, namely, only if there is a SAD

settled at smaller radii. Objects with a dead zone extending down to the star would have no trap. On the contrary, young stars producing jets require the presence of a JED in the inner disk region. In that case, the trap is located at the outer JED radius (the JED itself may extend down to the star with no impact on the trap). Note also that, since a JED is less dense than a SAD, it is unlikely that a dead zone would establish (J. Ferreira et al. 2006, in preparation).

The likely existence of such planetary traps in protoplanetary disks has important implications for the formation of giant planets. First, it constitutes a workaround to the timescale conflict between a solid core buildup (which is slow) and its migration to the central object (which would be fast, if the object was not stopped at a trap). Second, a large amount of solid embryos should accumulate at the trap location. This should speed up the buildup of a critical mass core ($M_p \simeq 15\ M_\oplus$), which could accrete the nebula gas and convert itself into a giant planet. The dynamics of the set of embryos trapped at the jump is, however, beyond the scope of this communication and will be presented in a forthcoming work.

We have seen in § 2 that the corotation torque value is boosted not only by the large surface density gradient but also by the alteration of the rotation profile, which yields a large gradient of B, with both large minimal and maximal values, since the gradient of B involves the second derivative of the angular velocity. One may wonder whether at a disk opacity transition, in which there is a disk temperature jump and hence a pressure gradient radial jump, the alteration of the rotation profile is sufficient to yield a peak value of the corotation torque that counteracts the Lindblad torque. We have undertaken subsidiary calculations in which we have a power-law surface density profile and a sound speed profile with a localized radial jump. We found that we need a jump of the aspect ratio of ~ 1.5 over $4H$ in order to halt migration. This ratio is too large and is unrealistic in a SAD. Indeed, in a standard accretion disk in which energy is transported vertically by radiative diffusion, the central temperature scales as $\tau^{1/8}$, where τ is the optical depth. As a consequence, even in the vicinity of an opacity transition, the temperature profile exhibits a smooth behavior and the corotation torque is not sufficiently strong to counterbalance the Lindblad torque. Nevertheless, Menou & Goodman (2004) have found that the opacity transitions may induce a significant reduction of the differential Lindblad torque, but they explicitly neglected the corotation torque in their study. It would be of interest to investigate whether the corotation torque boost at these locations can be sufficient to halt migration.

Remarkably, the scale height of a JED is always smaller than that of the SAD, so that the transition between these two flows naturally yields a jump in the disk aspect ratio. This is due to two effects. First, a JED feeds its jets with most of the released accretion power so that only a small fraction of it is radiated away at the disk surface: the disk is cooler. Second, in addition to gravity, the large-scale magnetic field vertically pinches the disk (Ferreira 1997).

We also stress that at the inner dust puffed-up rims of protoplanetary disks (Isella & Natta 2005), there can be a large radial gradient of the gas temperature, which may be sufficient to trap migrating planets.

We finally emphasize that the mechanism presented here does not allow low-mass objects to proceed inside of a cavity, but rather traps them on the cavity edge. This is quite different from what has been studied in the context of gap opening planets, which migrate farther inside until they reach the 2:1 resonance with the cavity edge (Kuchner & Lecar 2002).

---

[5] In fact, velocity shifts detected in jets are interpreted as being a rotation signature, which then allows one to derive the outer jet launching radius in the underlying accretion disk. This radius corresponds to our transition radius.

6. CONCLUSIONS

We have shown that the type I migration of $M_p < 15 \, M_\oplus$ planets can be halted at radially localized disk surface density jumps (the surface density being larger on the outside of the jump). Some turbulence is then required to prevent the corotation torque saturation. The latter tends to induce stochastic migration of the embryos and therefore tends to act against the trap. The lighter the disk, the easier it is to keep an embryo trapped, since its radial jitter over the timescale needed to reach torque convergence is small and can be confined to the vicinity of the trap stable fixed point. Inversely, the lighter the embryo, the more difficult it is to trap it: in the zero-mass limit, the embryo has no tidal torque and only feels the torque fluctuations arising from turbulence. We have shown that a jump with a large surface density ratio efficiently traps embryos above $1 \, M_\oplus$ up even in relatively massive disks, such as the MMSN at $r = 5$ AU, while shallow jumps (a 40% surface density increase over ~ 4 disk scale heights) will retain embryos of a few Earth masses and more only in light disks, such as the MMSN at $r = 0.1$ AU. We have illustrated by means of numerical simulations that a surface density jump traps infalling embryos and that it drives them along with it if it moves radially as the disk evolves. Such a jump can occur at different locations in a protoplanetary disk: it can be found at the transition between the standard accretion disk solution (SAD) and the jet-emitting disk (JED), thought to be at a distance 0.3 to 1–2 AU from the central object. It can also be found at the inner edge of a dead zone, where one expects a very large ratio of outer to inner surface densities. It may also be found at the outer edge of a protoplanetary gap if one giant planet already exists in the disk. We have stressed that these planetary traps have two important consequences: (1) they can hold the type I migration of protogiant cores over the timescale needed to overcome the critical mass ($\sim 15 \, M_\oplus$) over which rapid gas accretion begins onto these cores, which are then quickly converted into giant planets that should enter the slow, type II migration regime; and (2) as solid embryos accumulate at the trap, the buildup of critical cores should be faster than elsewhere in the disk. Finally, we mentioned that, although temperature radial jumps in principle also yield large peaks of the corotation torque, they are unlikely to be able to counteract the Lindblad torque by themselves, as the temperature gradients required for that are unrealistically large in a standard accretion disk.

APPENDIX

PRESCRIPTION FOR THE ONE-DIMENSIONAL CALCULATION OF THE PLANET SEMIMAJOR AXIS TIME EVOLUTION IN THE PRESENCE OF TORQUE FLUCTUATIONS

The planet semimajor axis is evolved in time using a Euler method:

$$a(t + \Delta t) = a(t) + \Delta t \frac{\Gamma_l + \Gamma_f}{2B[a(t)]a(t)}, \tag{A1}$$

where $a(t)$ is the planet semimajor axis at date t, Γ_l is the torque as measured in a laminar disk for a planet in circular orbit of radius a, linearly interpolated from the results displayed in either Figure 2a or 4a, Γ_f is the torque fluctuation due to turbulence, and where a Keplerian profile is assumed for B (this is grossly wrong as far as its radial derivative is concerned, as we saw in the main text, but this is largely sufficient for our purpose here). The torque fluctuation is evaluated as follows:

$$\Gamma_f = G\Sigma_m[a(t)]a(t)[2V - 1], \tag{A2}$$

where $\Sigma_m[a] = \max [\Sigma(r)]_{r \in [a-H, \, a+H]}$ and V is a random variable uniformly distributed over $[0, 1]$. The value of Γ_f is kept constant over t_c. We use the above prescription for $\Sigma_m[a]$, since the planet is located in a region where the surface density gradient is large. The largest torque fluctuations may arise from regions located within $a - H$ to $a + H$ from the central object and where the surface density may be significantly different from the one at the planet location. Each realization of the random variable is independent of the previous ones. We anticipate that the results should not depend on the torque fluctuation law, since the central limit theorem states that the cumulative torque law tends toward a normal law (Nelson 2005).

REFERENCES

Alibert, Y., Mordasini, C., Benz, W., & Winisdoerffer, C. 2005, A&A, 434, 343
Artymowicz, P. 2004, in ASP Conf. Ser. 324, Debris Disks and the Formation of Planets, ed. L. Caroff et al. (San Francisco: ASP), 39
Balbus, S. A., & Hawley, J. F. 1991, ApJ, 376, 214
Balmforth, N. J., & Korycansky, D. G. 2001, MNRAS, 326, 833
Coffey, D., Bacciotti, F., Woitas, J., Ray, T. P., & Eislöffel, J. 2004, ApJ, 604, 758
D'Angelo, G., Bate, M. R., & Lubow, S. H. 2005, MNRAS, 358, 316
Ferreira, J. 1997, A&A, 319, 340
Ferreira, J., & Pelletier, G. 1995, A&A, 295, 807
Fromang, S., Terquem, C., & Balbus, S. A. 2002, MNRAS, 329, 18
Gammie, C. F. 1996, ApJ, 457, 355
Goldreich, P., & Tremaine, S. 1979, ApJ, 233, 857
Hahn, J. M., & Ward, W. R. 1996, Lunar Planet. Sci. Conf., 27, 479
Hartigan, P., Edwards, S., & Ghandour, L. 1995, ApJ, 452, 736
Hartmann, L. 2001, Accretion Processes in Star Formation (Cambridge: Cambridge Univ. Press)
Isella, A., & Natta, A. 2005, A&A, 438, 899
Klahr, H. 2004, ApJ, 606, 1070
Korycansky, D. G., & Pollack, J. B. 1993, Icarus, 102, 150
Kuchner, M. J., & Lecar, M. 2002, ApJ, 574, L87
Li, H., Colgate, S. A., Wendroff, B., & Liska, R. 2001, ApJ, 551, 874
Li, H., Finn, J. M., Lovelace, R. V. E., & Colgate, S. A. 2000, ApJ, 533, 1023
Masset, F. S. 2000a, A&AS, 141, 165
———. 2000b, in ASP Conf. Ser. 219, Disks, Planetesimals, and Planets, ed. F. Garzón et al. (San Francisco: ASP), 75
———. 2001, ApJ, 558, 453
———. 2002, A&A, 387, 605
Masset, F. S., & Papaloizou, J. C. B. 2003, ApJ, 588, 494
Menou, K., & Goodman, J. 2004, ApJ, 606, 520
Nelson, R. P. 2005, A&A, 443, 1067
Nelson, R. P., & Papaloizou, J. C. B. 2004, MNRAS, 350, 849
Ogilvie, G. I., & Lubow, S. H. 2002, MNRAS, 330, 950

Pesenti, N., Dougados, C., Cabrit, S., Ferreira, J., Casse, F., Garcia, P., & O'Brien, D. 2004, A&A, 416, L9

Pollack, J. B., Hubickyj, O., Bodenheimer, P., Lissauer, J. J., Podolak, M., & Greenzweig, Y. 1996, Icarus, 124, 62

Tanaka, H., Takeuchi, T., & Ward, W. R. 2002, ApJ, 565, 1257

van Leer, B. 1977, J. Comput. Phys., 23, 276

Ward, W. R. 1986, Icarus, 67, 164

———. 1991, Lunar Planet. Sci. Conf., 22, 1463

———. 1992, Lunar Planet. Sci. Conf., 23, 1491

———. 1997, Icarus, 126, 261